Hydrogel-Based Actuators

Bioinspired Synergistic Fluorescence-Color-Switchable Polymeric Hydrogel Actuators

Shuxin Wei, Wei Lu,* Xiaoxia Le, Chunxin Ma, Han Lin, Baoyi Wu, Jiawei Zhang, Patrick Theato und Tao Chen*

Abstract: *Many living organisms have amazing control over their color, shape, and morphology for camouflage, communication, and even reproduction in response to interplay between environmental stimuli. Such interesting phenomena inspire scientists to develop smart soft actuators/robotics via integrating color-changing functionality based on polymer films or elastomers. However, there has been no significant progress in synergistic color-changing and shape-morphing capabilities of life-like material systems such as hydrogels. Herein, we reported a new class of bioinspired synergistic fluorescence-color-switchable polymeric hydrogel actuators based on supramolecular dynamic metal–ligand coordination. Artificial hydrogel apricot flowers and chameleons have been fabricated for the first time, in which simultaneous color-changing and shape-morphing behaviors are controlled by the subtle interplay between acidity/alkalinity, metal ions, and temperature. This work has made color-changeable soft machines accessible and is expected to hold wide potential applications in biomimetic soft robotics, biological sensors, and camouflage.*

Introduction

Many living organisms, including cephalopods, chameleons, frogs, and flowers, have excellent control over their color and morphology for camouflage, communication, and

[*] S. Wei, Dr. W. Lu, Dr. X. Le, H. Lin, B. Wu, Prof. J. Zhang, Prof. T. Chen
Key Laboratory of Marine Materials and Related Technologies
Zhejiang Key Laboratory of Marine Materials and Protective Technologies, Ningbo Institute of Materials Technology and Engineering
Chinese Academy of Sciences
Ningbo 315201 (China)
E-Mail: luwei@nimte.ac.cn
        tao.chen@nimte.ac.cn

S. Wei, Dr. W. Lu, Dr. X. Le, Prof. J. Zhang, Prof. T. Chen
School of Chemical Sciences
University of Chinese Academy of Sciences, Beijing 100049 (China)

Dr. C. Ma
State Key Laboratory of Marine Resources Utilization in South China Sea, Hainan University
Haikou 570228 (China)

Prof. P. Theato
Soft Matter Synthesis Laboratory, Institute for Biological Interfaces III
Karlsruhe Institute of Technology (KIT)
Herrmann-von-Helmholtz-Platz 1, 76344 Eggenstein-Leopoldshafen (Germany)

Supporting information and the ORCID identification number(s) for the author(s) of this article can be found under:
https://doi.org/10.1002/anie.201908437.

reproduction, in response to an interplay between various environmental stimuli.[1] These exciting phenomena inspired scientists to integrate color-shifting functionality in soft actuators, resulting in a multifunctional synergy to yield more powerful soft robotics (e.g., camouflaged robots).[1a,2] For example, Whitesides and co-workers[1a] have fabricated elegant color-changing soft machines for camouflage and display through integration of thin silicone sheets that contain microfluidic networks into pneumatic elastomer robots. Zhu et al.[2c] developed a humidity-responsive color-changing actuator by coating a perfluorosulfonic acid ionomer film with well-ordered SiO_2 nanoparticles encapsulated by PDMS (chromogenic photonic crystals). Ko et al.[2d] realized electrical stimuli-responsive simultaneous actuation motions and color-shifting functions of bilayer actuators, which were prepared by using low-density polyethylene film and poly(vinyl chloride) film, as well as percolation of silver nanowires that acted as a heater between the two films. These impressive advances have paved the way for the fabrication of biomimetic color-changing soft robotics and demonstrated their wide potential use in many different scientific areas.

However, these multifunctional actuators are primarily based on polymer films or elastomers. The synergetic color-changing and shape-morphing capabilities of living organisms have not been replicated by soft hydrogels. Compared to polymeric films and elastomers, polymeric hydrogels, featuring a three-dimensional hydrophilic network structure swollen by a large amount of water, show unique tissue-like mechanical properties and excellent biocompatibility.[3] Therefore, soft wet hydrogel-based anisotropic actuators with color-changing characteristics are much more similar to such natural creatures such as chameleons and flowers and thus hold great potential for applications in soft robotics, artificial muscles, biosensors, intelligent bionics, and smart valves.[4,5] Nevertheless, despite the great progress made recently in hydrogel actuators with complex 3D deformation,[6,7] it is still quite challenging to achieve synergetic color-changing and 3D shape-morphing in one single hydrogel system.

Very recently, we made an important attempt in combining a thermoresponsive graphene oxide–poly(*N*-isopropylacrylamide) hydrogel layer with a pH-responsive perylene bisimide (PBI)-functionalized fluorescent hydrogel layer to fabricate anisotropic actuators with „on–off" fluorescence switching behavior.[8] In this work, the developed system can only emit one fluorescence color and the fluorescence change is achieved only by a physical folding/unfolding of the hydrogel actuator; this color change is far inferior to that of
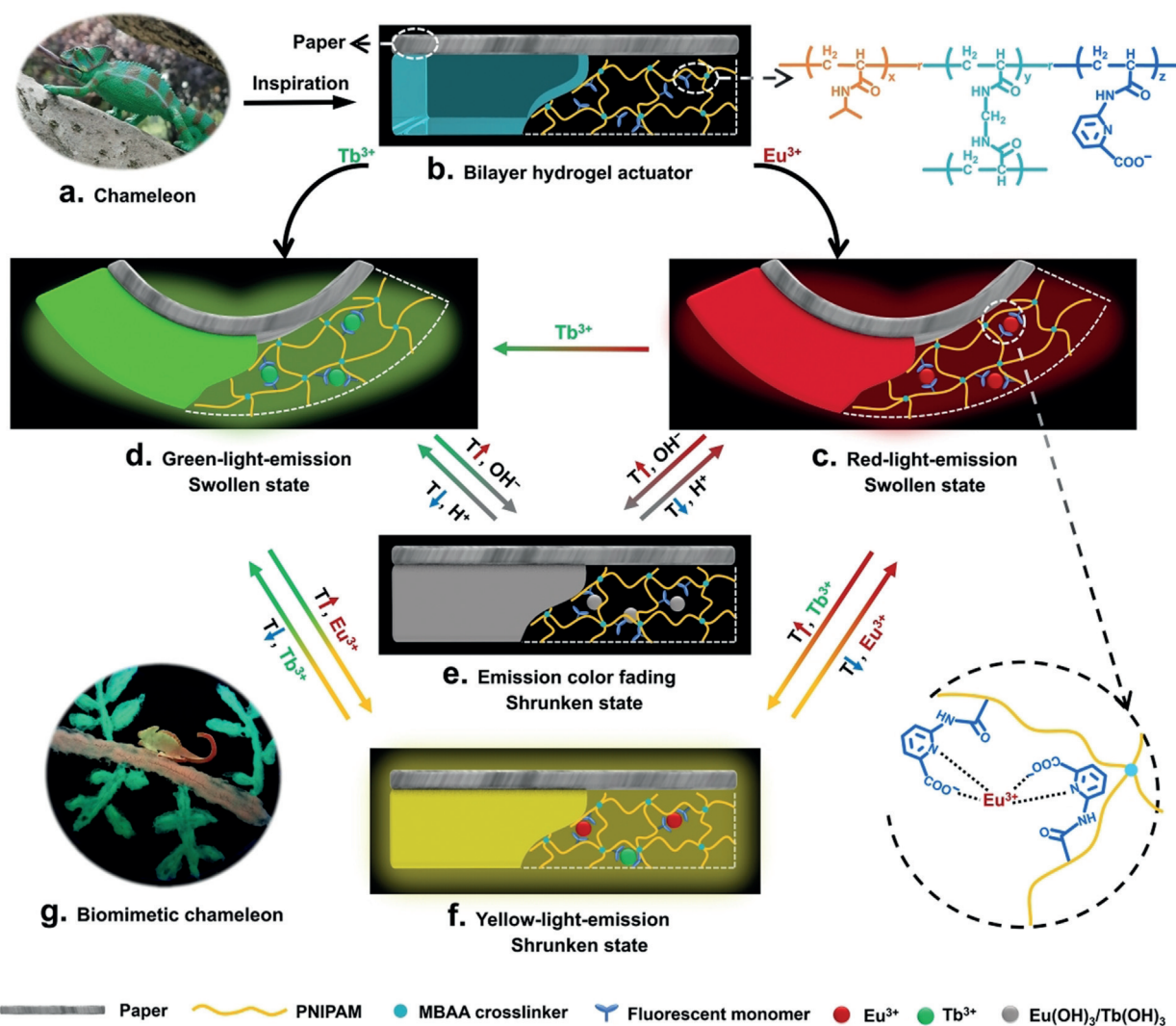
Scheme 1. Schematic illustration of the bioinspired synergetic fluorescence-color-switchable polymeric hydrogel actuators. a) Photo of a chameleon model. b) Illustration of the bilayer hydrogel actuators and their molecular structure. c) Red-light-emitting actuator in the swollen state which was prepared by immersing the bilayer hydrogel in Eu^{3+} solution at 18°C. d) Green-light-emitting actuator in the swollen state which was prepared by immersing the bilayer hydrogel or red-light-emitting hydrogel actuator in Tb^{3+} solution at 18°C. e) Nonfluorescent hydrogel actuator in the shrunken state which was obtained by immersing a red- or green-light-emitting actuator in NaOH solution at 40°C. The fluorescence and shape could be recovered by adding acid at 18°C. f) Yellow-light-emitting hydrogel actuator in the shrunken state which was obtained by immersing the red-light-emitting actuator in Tb^{3+} solution at 40°C or the green-light-emitting actuator in Eu^{3+} solution at 40°C. These processes are highly reversible. g) Image of biomimetic chameleon-shaped soft actuator with camouflaging ability, which was taken under a 254 nm UV lamp.

natural creatures like chameleons that can exhibit variations of skin color in different surroundings.

We herein utilized dynamic metal–ligand coordination[9] to construct smart multicolor fluorescent polymeric hydrogels, which can be used to fabricate anisotropic soft actuators showing chameleon-inspired simultaneous color-shifting and shape-morphing behavior (Scheme 1a). The hydrogels were prepared by radical copolymerization of potassium 6-acryl-amidopicolinate (K6APA) and *N*-isopropylacrylamide (NI-PAM) (Scheme 1b), followed by coordination with Eu^{3+} or Tb^{3+} ions. The hydrogels display the characteristic intense red- and green-light emission of Eu^{3+} and Tb^{3+}, respectively,

and their emission color can be facilely adjusted in response to changes in acidity/alkalinity or metal ions. Bilayer soft actuators were then prepared by bonding the developed multicolor fluorescent hydrogels with pan paper (Scheme 1b–f). As proof of concept, an artificial apricot blossom with synergetic red-color-fading and blooming behavior was demonstrated in response to the interplay between temperature and acidity/alkalinity stimuli. Furthermore, smart chameleon-shaped soft robots with camouflaging ability were developed (Scheme 1g), which display simultaneous body movement and change in skin color from red to yellow or green, similar to that of the natural chameleons.

Results and Discussion

The key step in preparing multicolor fluorescent hydrogels is the design of the ligand monomer 6-acrylamidopicolinic acid (6APA), which was synthesized by an amidation reaction of methyl 6-aminopyridine-2-carboxylate with acryloyl chloride and subsequent hydrolysis of the methyl ester (Figure S1). The chemical structure of 6APA was verified by ^{1}H and ^{13}C NMR spectroscopy (Figure 1a and Figure S2). 6APA is soluble in DMSO and DMF, but is nearly insoluble in water. In order to introduce the pyridine carboxylate ligand evenly into the hydrogels, the corresponding potassium salt, potassium 6-acrylamidopicolinate (K6APA), was prepared. Job plot investigation indicates that K6APA forms a 2:1 complex with Eu^{3+} or Tb^{3+} ions (Figure 1b,c).[10] Consequently, a PNIPAM-K6APA hydrogel was prepared by photoinduced radical polymerization of NIPAM, methylenebisacrylamide (MBAA) crosslinker, and K6APA using I2959 as the photoinitiator (Figure 1d). The as-prepared

hydrogel is highly transparent (Figure S3) but nearly non-fluorescent. Since pyridine carboxylate groups are known to serve as sensitizers to significantly increase the emission intensity of Eu^{3+} or Tb^{3+} ions through resonance energy transfer (RET) (Figures S4–S7),[11] red- and green-light-emitting hydrogels (Eu-PNIPAM-K6APA and Tb-PNIPAM-K6APA) were then produced by immersing the as-prepared PNIPAM-K6APA hydrogels into aqueous Eu^{3+} and Tb^{3+} solutions, respectively (Figure S4). Both Eu-PNIPAM-K6APA and Tb-PNIPAM-K6APA hydrogels are still highly transparent under daylight (Figure S3). However, they have higher modulus and toughness than PNIPAM-K6APA, which clearly demonstrates the formation of dynamic, metal–ligand coordination crosslinks (Figure 1e and Figure S8). Interestingly, when the PNIPAM-K6APA hydrogel is immersed into mixed solutions of Eu^{3+} and Tb^{3+}, multicolor fluorescent hydrogels were obtained. As shown in Figure 1f,g, the hydrogel emission color can be modulated by varying the Eu^{3+}/Tb^{3+} molar ratio of the mixed solutions. Fluorescence
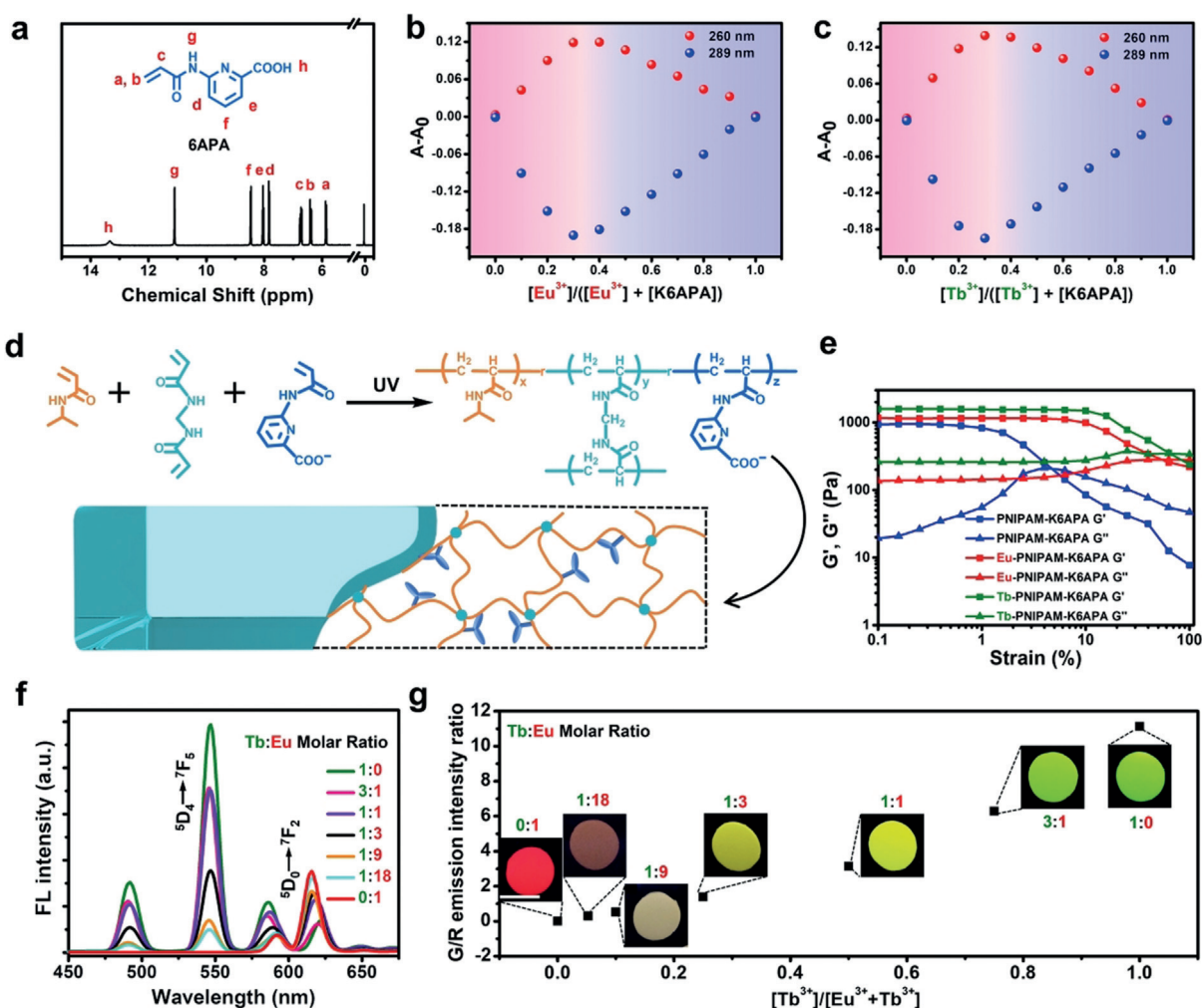

Figure 1. a) The ^{1}H NMR spectrum of the fluorescent monomer 6APA. b,c) Job plots of potassium 6-acrylamidopicolinate (K6APA), which suggest that K6APA forms a 2:1 complex with Eu^{3+} or Tb^{3+} ions. d) Illustration of the PNIPAM-K6APA hydrogel and its chemical structure. e) The rheology properties of PNIPAM-K6APA, Eu-PNIPAM-K6APA, and Tb-PNIPAM-K6APA hydrogels at an oscillation frequency of 1 Hz. f) Fluorescence spectra ($\lambda_{ex} = 254$ nm) of multicolor fluorescent hydrogels, which are prepared by immersing the PNIPAM-K6APA hydrogel into mixed solutions of Eu^{3+} and Tb^{3+}. g) The green/red (G/R) emission intensity ratio as a function of the Tb^{3+}/Eu^{3+} molar ratio (0:1, 1:18, 1:9, 1:3, 1:1, 3:1, 1:0) and the corresponding photographs. Scale bar is 1 cm. All photos were taken under a 254 nm UV lamp.

spectroscopy investigation revealed that the intensity of the green band at 547 nm increased at the cost of the intensity of the red band at 617 nm upon an increase in the Tb^{3+}/Eu^{3+} molar ratio.

Next, anisotropic bilayer actuators were prepared by employing these multicolor fluorescent hydrogels as the actuating layer and pan paper as a passive layer (Figures S9 and S10). Their anisotropic actuation motion was primarily induced by the large mismatch in modules and swelling ability of these two layers (Figure S11). SEM images demonstrate the typical and expected bilayer structure, which is fixed by the interpenetrating network between the paper fibers and the hydrogel network (Figure 2 a,b and Figures S12 and S13). The bilayer hydrogels can be facilely tailored to fabricate anisotropic actuators with various shapes (Figure S14). For example, the straight nonfluorescent PNIPAM-K6APA ac-

tuator will gradually swell and curl to a red-light-emitting circle-shaped Eu-PNIPAM-K6APA hydrogel actuator when placed into an aqueous Eu^{3+} solution at 18°C. Note that the fluorescence spectra (Figure S15) and maximum emission intensities (Figure S16) recorded at both the hydrogel and paper sides of the Eu-PNIPAM-K6APA actuator are still comparable within experimental error, demonstrating that the porous paper layer almost has no effect on the light emission and color visualization of the developed actuators. Moreover, since the fluorescent Eu-K6APA complex is very sensitive to acidity/alkalinity changes, the red-light emission of the Eu-PNIPAM-K6APA actuator gradually fades upon exposure to alkaline environment (Figure 2 c,d and Figure S17), while retreatment with acid solutions can recover the intense red-light emission (Figure 2 c and Figure S17). The red-color-fading time of the Eu-PNIPAM-K6APA actuator is
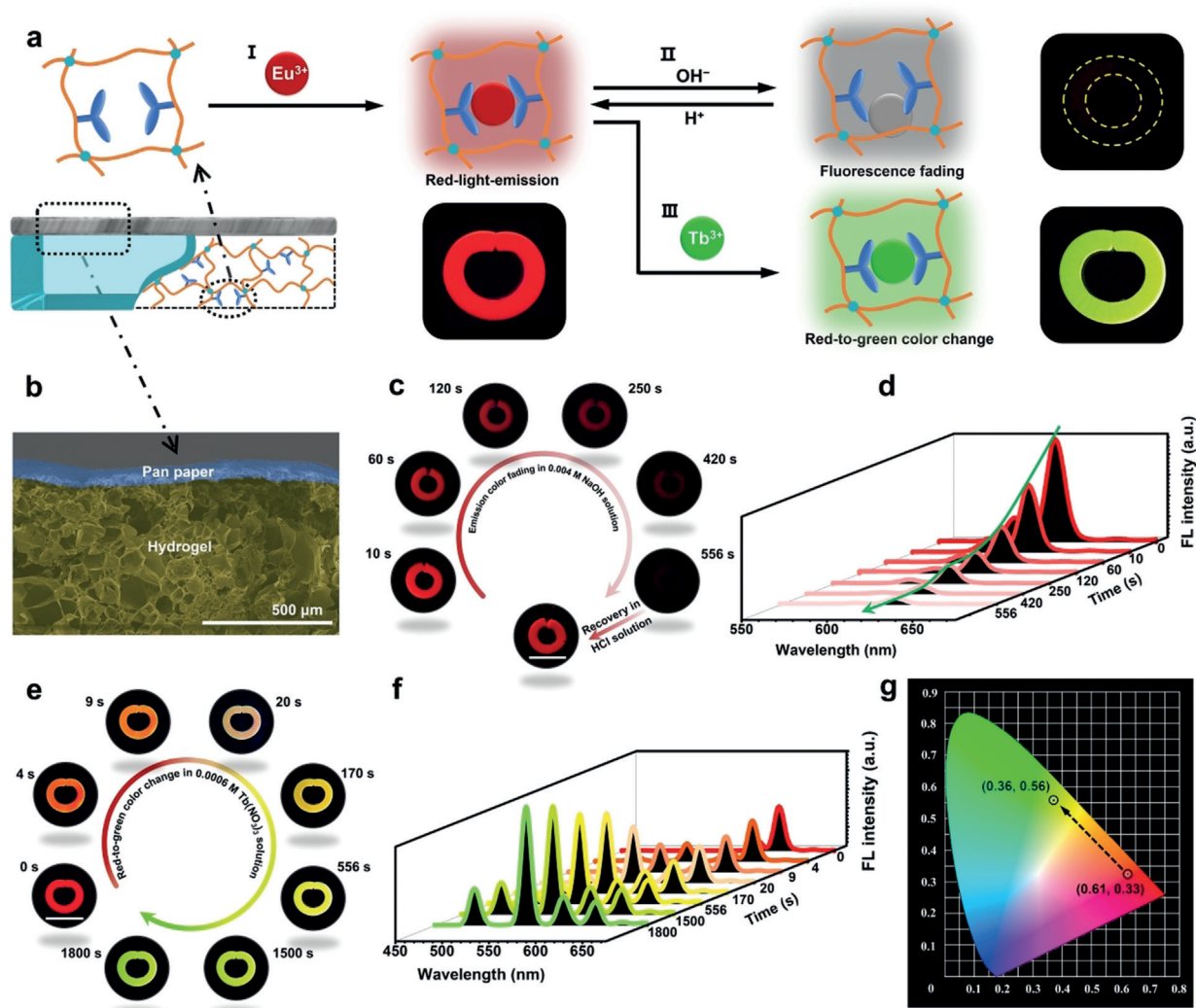

Figure 2. Stimuli-responsive fluorescence-color-changing actuators. a) Fabrication of the Eu-PNIPAM-K6APA actuator as well as OH⁻- induced color fading and Tb-triggered red-to-green color change. b) Cross-section SEM image of the actuator. c,d) Photographs (c) and fluorescence spectra ($\lambda_{ex} = 254$ nm) (d) of the fluorescence fading of the Eu-PNIPAM-K6APA actuator in 0.004 M NaOH aqueous solution and fluorescence recovery state in 0.001 M HCl aqueous solution. e,f) Photographs (e) and fluorescence spectra (f) of the fluorescent color change of the Eu-PNIPAM-K6APA actuator in 0.0006 M Tb(NO₃)₃ aqueous solution. g) CIE (1931) coordinate diagrams for 0 s and 1800 s states of Eu-PNIPAM-K6APA actuator during the fluorescence-color-changing process. Scale bars in digital photos are 1 cm. All of the photographs were taken under a 254 nm UV lamp.

dependent on OH⁻ concentration (Figure S18), because the process is typically diffusion-controlled. Similar acidity/alkalinity-triggered fluorescence-color-fading phenomenon is also observed for the Tb-PNIPAM-K6APA actuator (Figures S18 and S19). Additionally, the more interesting emission-color change of the Eu-PNIPAM-K6APA actuator was demonstrated in response to Tb^{3+} ions stimuli. As exhibited in Figure 2e, a remarkable color change from red to yellow to green was observed when the Eu-PNIPAM-K6APA actuator was placed in Tb^{3+} solutions. It is because Eu^{3+} ions in the red-light-emitting Eu-K6APA complex will be gradually replaced by the excess Tb^{3+} ions to form green-light-emitting Tb-K6APA complex. This is evidenced by the results that the emission band centered at 547 nm gradually increases and emission band around 617 nm decreases over time (Figure 2 f,g and Figure S20). The emission-color-changing process is also diffusion-controlled and thus could be adjusted by varying Tb^{3+} concentration (Figure S21).

For a quantitative investigation of the shape deformation of the actuators, hydrogel stripes at 18°C bent in the original arc shape with the hydrogel on the outer face were chosen as the basic model and the change in the bending angle (θ) was measured (Figure 3a). As summarized in Figure 3b,c, the bending angle of a Eu-PNIPAM-K6APA actuator stripe rapidly decreased from ≈303° (8 s) to ≈13° (211 s) within 203 s in hot water at 40°C and then increased to ≈355° again within 67 min in cold water at 18°C due to thermoresponsive nature of the fluorescent hydrogel layer.[12] The unbending
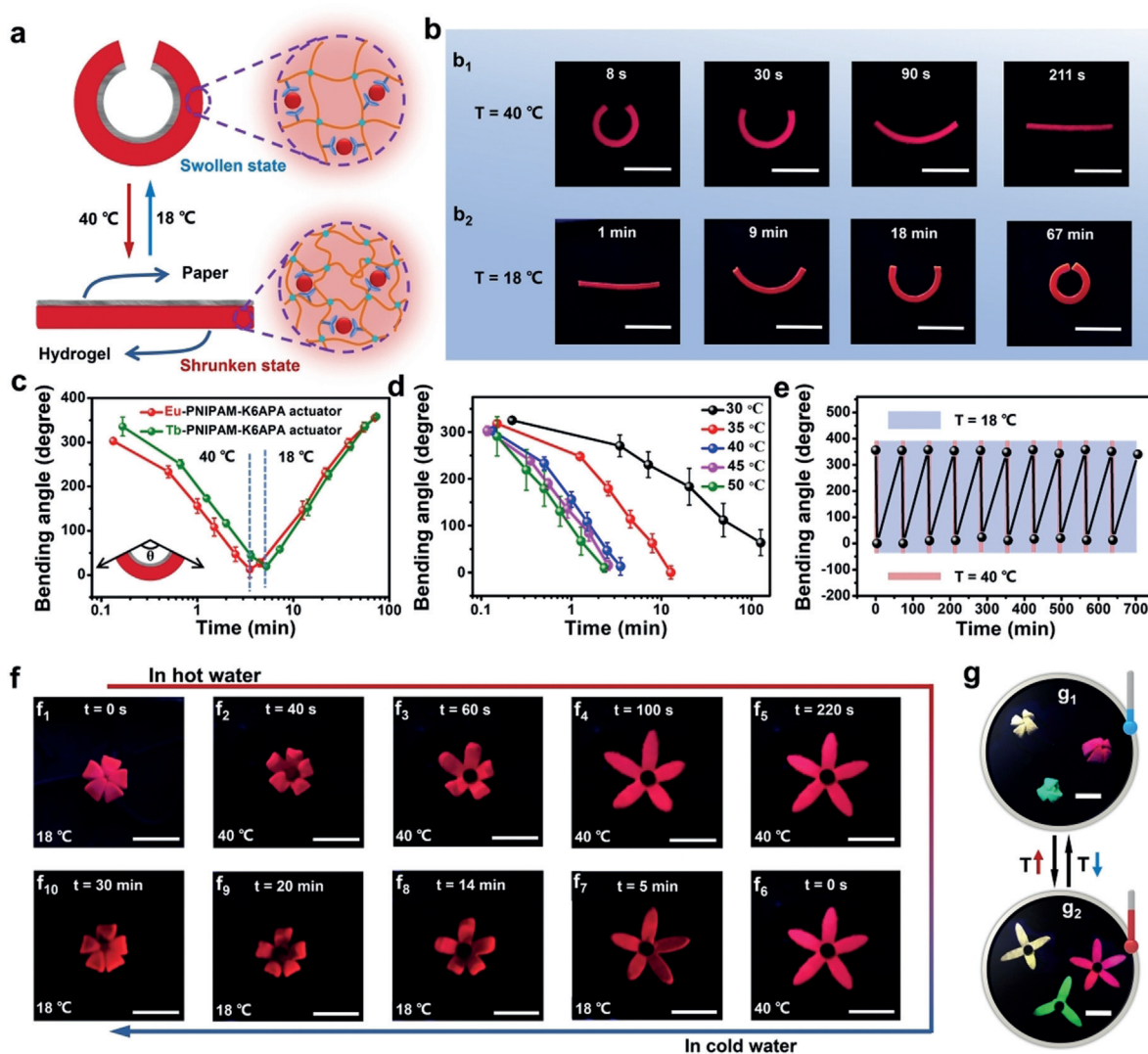
Figure 3. Thermoresponsive shape deformation of the actuator. a) Schematic representation of the bending behavior of Eu-PNIPAM-K6APA actuator from its arc-shaped original state. b) Thermotriggered unbending and bending behavior of the Eu-PNIPAM-K6APA actuator stripe. c) Bending angles of Eu-PNIPAM-K6APA and Tb-PNIPAM-K6APA actuators as a function of time. d) Time-dependent bending angles of Eu-PNIPAM-K6APA actuators, which are recorded in water with different temperature. e) Cyclic actuating process of the Eu-PNIPAM-K6APA actuator which was triggered by temperature change between 18°C and 40°C. f) Images showing the flower-shaped Eu-PNIPAM-K6APA actuator that bloomed in 40°C water and closed in 18°C water. The original state of the flower-shaped actuator was programmed as a „bud" through anisotropic swelling in cold water (18°C). g) Images of thermotriggered „bouquets of flowers" based on multi-emission-color hydrogel-based artificial flowers with different numbers of petals. Scale bars are 1 cm. All fluorescent photos were taken under a 254 nm UV lamp.

speed could be adjusted by varying the temperature of the water (Figure 3 d). The thermotriggered shape deformation behavior was highly reversible and can be repeated for at least 10 cycles without significant bending angle changes (Figure 3 e and Table S1), indicating the good stability of the hydrogel stripes. Similar heat-triggered shape changes were also observed for Tb-PNIPAM-K6APA actuators (Figures S22 and S23 and Table S2). Furthermore, actuators with more complex 3D shape transformation were also demonstrated. As can be seen from Figure 3 f, a flower-shaped Eu-PNIPAM-K6APA actuator with five petals was programmed as a dormant „bud" (Figure 3 f_1) through anisotropic swelling in cold water (18 °C) as the original state. After the actuator bud was placed into 40 °C hot water, shrinkage of the hydrogel side led to the gradual blooming of our flower-shaped actuator over time (Figure 3 f_1–f_5). Gradual closing of the flower could be triggered upon retreatment in 18 °C cold water (Figure 3 f_6–f_{10}). On the basis of these results, beautiful images of „bouquets of flowers" were demonstrated by the developed multi-emission-color hydrogel-based artificial flowers with different numbers of petals (Figure 3 g and Figures S24 and S25).

Many natural plants display intriguing changes in appearance. For example, apricot blossoms typically bloom and the red color fades simultaneously (Figure 4 a) for attracting pollinators and promoting reproduction, in response to the interplay between changes in temperature and acidity/alkalinity. This interesting behavior of the natural flower encouraged us to fabricate artificial counterparts. To this end, a red-color hydrogel apricot flower having five petals was prepared using the Eu-PNIPAM-K6APA hydrogel actuator and was then pre-swollen in 18 °C cold water to produce the flower bud. Like the natural apricot blossom, the red-colored flower bud remains closed at low temperature and neutral conditions (18 °C, deionized water) but gradually opens to a colorless blooming flower at high temperature and alkaline conditions (40 °C, 0.05 M NaOH solution, Figure 4 b_1–b_5). Either high temperature or alkaline environment alone cannot trigger the simultaneous color change and blooming behavior of our artificial flower. In other words, it is the subtle interplay between temperature and acidity/alkalinity variation that causes the functional synergy of color and shape change. As expected, simultaneous recovery of the red color and the bud shape could be triggered upon exposure to cold acidic solutions (Figure 4 b_6–b_{10}). The whole process could be repeated many times due to the highly reversible nature of both Eu^{3+} coordination and PNIPAM phase transition. Further, synergetic red-color-deepening and flower-blooming behaviors were also realized using the Eu-PNIPAM-K6APA actuator, in response to combined temperature and acidity/alkalinity stimuli (Figure 4 c,d).

In addition to natural plants, many animals such as chameleons change the color of their skin and their body shape or posture for the purpose of camouflage or communication depending on environmental temperature, light, or even mood.[13] For example, they can adapt their body color to match the surrounding environment (such as trees, flowers, plants, etc.) in order to conceal themselves. We attempted to mimic these interesting behaviors in artificial systems by using

the developed multicolor fluorescent hydrogel actuators. As a proof-of-concept, a chameleon-shaped soft robot was prepared by preshrinking the Eu-PNIPAM-K6APA bilayer hydrogel actuator in 40 °C hot water. The artificial chameleon was initially red and flat, which is in high contrast to the background of green branches and leaves we had drawn in the background using luminous paint. When cold Tb^{3+} solution (18 °C) is applied dropwise to the head of chameleon-shaped soft robot, the gradual diffusion of Tb^{3+} ions into the hydrogel matrix resulted in the gradual red-to-green color change from the head to the tail, accompanied by a noticeable body movement (Figure 5 a). As a result, our biomimetic hydrogel chameleon finally merged unobtrusively with the background, just like a real chameleon. Similarly, the color of the whole artificial chameleon changed gradually from red to green after being immersed into cold Tb^{3+} solution (18 °C), which contained green hydrogel leaves of Tb-PNIPAM-K6APA hydrogels (Figure 5 b). Another typical behavior of chameleons is mood-triggered synergistic change in skin color and posture for the purpose of communication. For example, when chameleons want to attack, their body color will darken. To this end, a pair of green- and red-light-emitting chameleon-shaped hydrogel actuators were fabricated to imitate the mood-triggered synergistic color-changing and shape-morphing behaviors of chameleons (Figure S26). In this way, chameleon-shaped soft hydrogel robots with camouflage and communication capabilities (although not perfect) are demonstrated for the first time, paving the road for accessible color-changing soft machines that are expected to be potentially useful to many different scientific areas.

Conclusion

In summary, we have reported a robust anisotropic soft actuator based on smart multicolor fluorescent Eu/Tb-PNIPAM-K6APA hydrogels via dynamic metal complexation, which can mimic synergetic color-changing and shape-morphing functions of some natural flowers and animals in response to a subtle interplay of various environmental stimuli (e.g., temperature, acidity/alkalinity). Benefitting from the dynamic nature of metal–ligand (Eu/Tb-K6APA) coordination, a remarkable emission color change of the actuators is facilely controlled by environmental stimuli such as acidity/alkalinity change and metal ions. In addition, reversible complex 3D deformations of the actuators were also demonstrated based on a thermotriggered inhomogeneous swelling that resulted in an overall bending motion. On the basis of these results, it is quite feasible to employ multiple stimuli to combine and optimize 3D shape deformation and multi-emission-color-switching functions into one single hydrogel system. As a proof of concept, an apricot-blossom-inspired artificial hydrogel flower was demonstrated for the first time, whose simultaneous color fading and blooming behaviors are dictated by the delicate interplay between temperature and acidity/alkalinity change. Furthermore, chameleon-shaped soft hydrogel robots were fabricated, which are capable of mimicking the synergetic skin color change and body movement of natural chameleons to realize camouflage. The
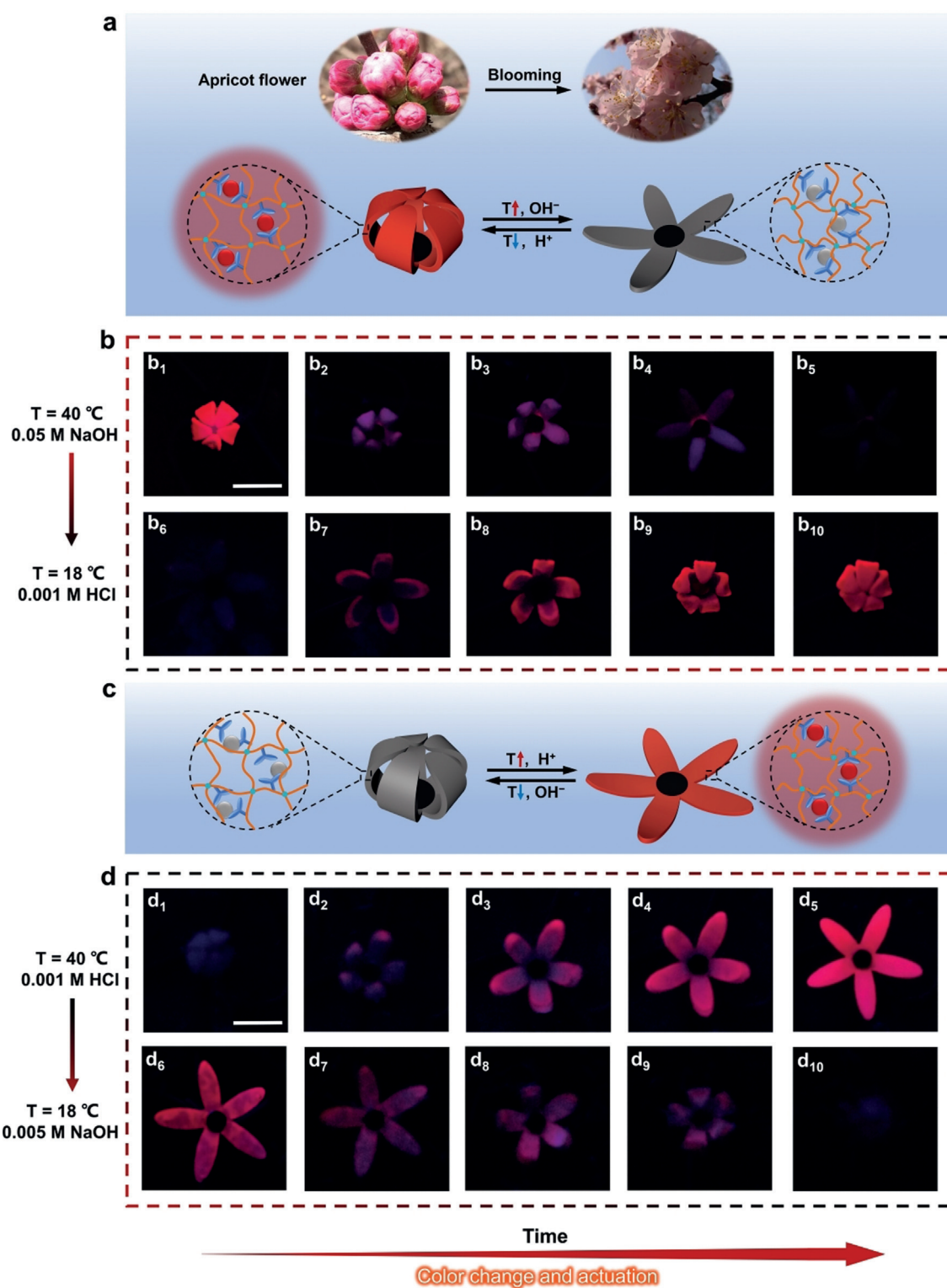
Figure 4. Synergetic color-changing and shape-deformation capabilities of Eu-PNIPAM-K6APA actuator-based artificial apricot flowers in response to the subtle interplay between temperature and acidity/alkalinity change. a,b) Images of natural apricot blossoms that display simultaneous blooming and color-fading behaviors, as well as schematic illustration and images of artificial hydrogel apricot flowers showing simultaneous color-switching and 3D complex shape deformation. b_1–b_5 show the blooming process accompanied by red-color fading, while b_6–b_{10} show the closing process with red-color recovery. c,d) Schematic illustration and images of artificial hydrogel apricot flowers showing simultaneous color-switching and 3D complex shape deformation. d_1–d_5 show the blooming process accompanied by red-color deepening, while d_6–d_{10} show the closing process with red-color fading. Scale bars are 1 cm. All the fluorescent photos were taken under a 254 nm UV lamp.
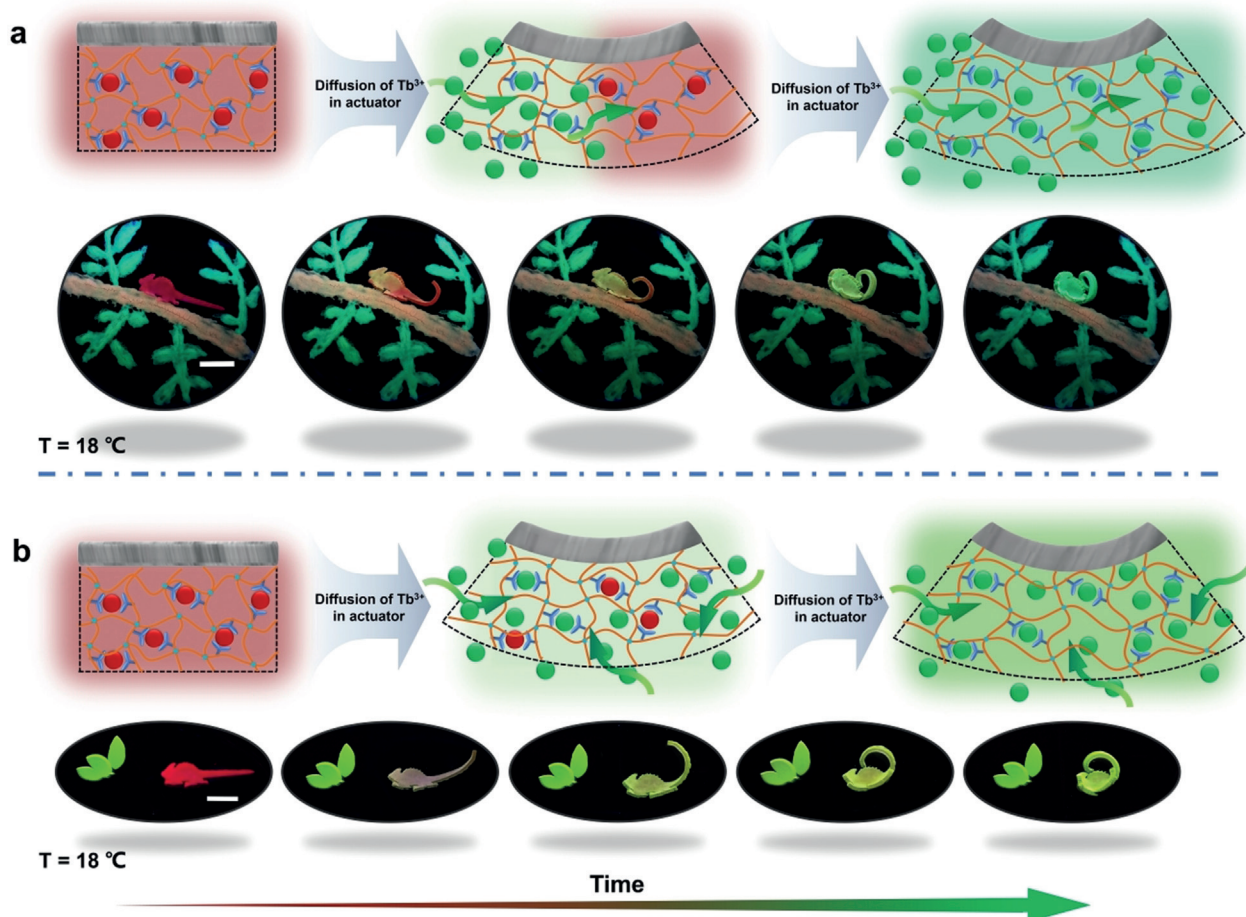
Figure 5. Synergetic color-changing and shape-morphing behaviors of biomimetic Eu-PNIPAM-K6APA hydrogel chameleons to realize camouflage capacity. a) Illustration and images showing simultaneous body deformation and color change of artificial hydrogel chameleons. $Tb(NO_3)_3$ aqueous solution (0.0006 M, 18°C) was continuously applied to the head of the chameleons to let Tb^{3+} ions diffuse into the hydrogel matrix from head to tail. Finally, high-concentration Tb^{3+} solution (0.1 M, 18°C) was added to deepen the green fluorescence of the chameleon-shaped hydrogel, making it merge into its surroundings. The background of branches and leaves was drawn with luminous paint. b) Illustration and images showing simultaneous body deformation and color-changing of the whole hydrogel chameleons. The actuator was immersed in 0.0006 M $Tb(NO_3)_3$ aqueous solution at 18°C to let Tb^{3+} ions diffuse into the hydrogel matrix. The green leaves were made by Tb-PNIPAM-K6APA hydrogels. The original state of the biomimetic chameleon was programmed to the shrunken state in hot water (40°C). Scale bars are 1 cm. All the fluorescent photos were taken under a 254 nm UV lamp.

proposed strategy has made color-changeable soft machines accessible and is expected to hold wide potential for applications in biomimetic soft robotics, biological sensors, visual detection/display, and camouflage applications.

Conflict of interest

The authors declare no conflict of interest.

[1] a) S. A. Morin, R. F. Shepherd, S. W. Kwok, A. A. Stokes, A. Nemiroski, G. M. Whitesides, *Science* **2012**, *337*, 828; b) J. Teyssier, S. V. Saenko, D. van der Marel, M. C. Milinkovitch, *Nat. Commun.* **2015**, *6*, 6368; c) L. M. Mäthger, S. L. Senft, M. Gao, S. Karaveli, G. R. R. Bell, R. Zia, A. M. Kuzirian, P. B. Dennis, W. J. Crookes-Goodson, R. R. Naik, G. W. Kattawar, R. T. Hanlon, *Adv. Funct. Mater.* **2013**, *23*, 3980.

[2] a) Y. X. Shang, Z. Y. Chen, F. F. Fu, L. Y. Sun, C. M. Shao, W. Jin, H. Liu, Y. J. Zhao, *ACS Nano* **2019**, *13*, 796; b) F. F. Fu, L. R. Shang, Z. Y. Chen, Y. R. Yu, Y. J. Zhao, *Sci. Robot.* **2018** https://doi.org/10.1126/scirobotics.aar8580; c) J. K. Mu, G. Wang, H. P. Yan, H. Y. Li, X. M. Wang, E. L. Gao, C. Y. Hou, A. T. C. Pham, L. J. Wu, Q. H. Zhang, Y. G. Li, Z. P. Xu, Y. Guo, E. Reichmanis, H. Z. Wang, M. F. Zhu, *Nat. Commun.* **2018**, *9*, 590; d) H. Kim, H. Lee, I. Ha, J. Jung, P. Won, H. Cho, J. Yeo, S. Hong, S. Han, J. Kwon, K.-J. Cho, S. H. Ko, *Adv. Funct. Mater.* **2018**, *28*, 1801847.

[3] a) Y. Y. Yang, X. Wang, F. Yang, L. N. Wang, D. C. Wu, *Adv. Mater.* **2018**, *30*, 1707071; b) H. Z. Kang, A. C. Trondoli, G. Zhu, Y. Chen, Y. J. Chang, H. Liu, Y. F. Huang, X. Zhang, W. Tan, *ACS Nano* **2011**, *5*, 5094; c) A. F. Greene, M. K. Danielson, A. O. Delawder, K. P. Liles, X. S. Li, A. Natraj, A. Wellen, J. C. Barnes, *Chem. Mater.* **2017**, *29*, 9498; d) F. Liu, M. W. Urban, *Prog. Polym. Sci.* **2010**, *35*, 3; e) H. Yang, C. H. Li, M. Yang, Y. D. Pan, Q. F. Yin, J. D. Tang, H. J. Qi, Z. G. Suo, *Adv. Funct. Mater.* **2019**, 1901721; f) T. Matsuda, R. Kawakami, R. Namba, T. Nakajima, J. P. Gong, *Science* **2019**, *363*, 504; g) Z. Y. Lei, Q. K. Wang, S. T. Sun, W. C. Zhu, P. Y. Wu, *Adv. Mater.* **2017**, *29*, 1700321; h) W. Q. Kong, C. W. Wang, C. Jia, Y. D. Kuang, G. Pastel, C. J. Chen, G. G. Chen, S. M. He, H. Huang, J. H. Zhang, S. Wang, L. B. Hu, *Adv. Mater.* **2018**, *30*, 1801934; i) X. F. Yang, G. Q. Liu, L. Peng, J. H. Guo, L. Tao, J. Y. Yuan, C. Y. Chang, Y. Wei, L. N. Zhang, *Adv. Funct. Mater.* **2017**, *27*, 1703174; j) L.-W. Xia, R. Xie, X.-J. Ju, W. Wang, Q. M. Chen, L.-Y. Chu, *Nat. Commun.* **2013**, *4*, 2226; k) C. D. Sorrell, M. C. D. Carter, M. J. Serpe, *Adv. Funct. Mater.* **2011**, *21*, 425; l) X. Li, M. J. Serpe, *Adv. Funct. Mater.* **2014**, *24*, 4119.

[4] a) S. M. Mirvakili, I. W. Hunter, *Adv. Mater.* **2018**, *30*, 1704407; b) H. Yuk, B. Y. Lu, X. H. Zhao, *Chem. Soc. Rev.* **2019**, *48*, 1642; c) H. Yuk, S. Lin, C. Ma, M. Takaffoli, N. X. Fang, X. H. Zhao, *Nat. Commun.* **2017**, *8*, 14230; d) X. Y. Liu, T.-C. Tang, E. Tham, H. Yuk, S. Lin, T. K. Lu, X. H. Zhao, *Proc. Natl. Acad. Sci. USA* **2017**, *114*, 2200; e) H. L. Lim, Y. Hwang, M. Kar, S. Varghese, *Biomater. Sci.* **2014**, *2*, 603; f) Y. Zhou, A. W. Hauser, N. P. Bende, M. G. Kuzyk, R. C. Hayward, *Adv. Funct. Mater.* **2016**, *26*, 5447; g) Y. C. Zhang, J. X. Liao, T. Wang, W. X. Sun, Z. Tong, *Adv. Funct. Mater.* **2018**, *28*, 1707245; h) W. N. Xu, D. H. Gracias, *ACS Nano* **2019**, *13*, 4883; i) C. Wang, X. Liu, V. Wulf, M. Vazquez-Gonzalez, M. Fadeev, I. Willner, *ACS Nano* **2019**, *13*, 3424; j) Z. F. Sun, Y. Yamauchi, F. Araoka, Y. S. Kim, J. Bergueiro, Y. Ishida, Y. Ebina, T. Sasaki, T. Hikima, T. Aida, *Angew. Chem. Int. Ed.* **2018**, *57*, 15772; *Angew. Chem.* **2018**, *130*, 15998; k) M. J. Liu, Y. Ishida, Y. Ebina, T. Sasaki, T. Hikima, M. Takata, T. Aida, *Nature* **2015**, *517*, 68; l) Y. S. Kim, M. J. Liu, Y. Ishida, Y. Ebina, M. Osada, T. Sasaki, T. Hikima, M. Takata, T. Aida, *Nat. Mater.* **2015**, *14*, 1002; m) Y. J. Sun, L. F. Chen, Y. Jiang, X. Zhang, X. K. Yao, S. Soh, *Mater. Horiz.* **2019**, *6*, 160.

[5] a) A. Mourran, H. Zhang, R. Vinokur, M. Möller, *Adv. Mater.* **2017**, *29*, 1604825; b) H. L. Qin, T. Zhang, N. Li, H.-P. Cong, S.-H. Yu, *Nat. Commun.* **2019**, *10*, 2202; c) Y. J. Jiang, L. M. Korpas, J. R. Raney, *Nat. Commun.* **2019**, *10*, 128; d) T. Ishiwata, K. Kokado, K. Sada, *Angew. Chem. Int. Ed.* **2017**, *56*, 2608; *Angew. Chem.* **2017**, *129*, 2652; e) S. Ikejiri, Y. Takashima, M. Osaki, H. Yamaguchi, A. Harada, *J. Am. Chem. Soc.* **2018**, *140*, 17308; f) T. Hessberger, L. B. Braun, R. Zentel, *Adv. Funct. Mater.* **2018**, *28*, 1800629; g) A. Choe, J. Yeom, R. Shanker, M. P. Kim, S. Kang, H. Ko, *NPG Asia Mater.* **2018**, *10*, 912; h) S. M. Chin, C. V. Synatschke, S. P. Liu, R. J. Nap, N. A. Sather, Q. F. Wang, Z. Alvarez, A. N. Edelbrock, T. Fyrner, L. C. Palmer, I. Szleifer, M. Olvera de la Cruz, S. I. Stupp, *Nat. Commun.* **2018**, *9*, 2395.

[6] a) Z. L. Wu, M. Moshe, J. Greener, H. Therien-Aubin, Z. H. Nie, E. Sharon, E. Kumacheva, *Nat. Commun.* **2013**, *4*, 1586; b) H. Thérien-Aubin, Z. L. Wu, Z. H. Nie, E. Kumacheva, *J. Am. Chem. Soc.* **2013**, *135*, 4834; c) R. Kempaiah, Z. H. Nie, *J. Mater. Chem. B* **2014**, *2*, 2357; d) W. X. Fan, C. Y. Shan, H. Y. Guo, J. W. Sang, R. Wang, R. R. Zheng, K. Y. Sui, Z. H. Nie, *Sci. Adv.* **2019**, *5*, eaav7174; e) H. L. Cui, N. Pan, W. X. Fan, C. Z. Liu, Y. H. Li, Y. Z. Xia, K. Y. Sui, *Adv. Funct. Mater.* **2019**, *29*, 1807692; f) A. Nishiguchi, A. Mourran, H. Zhang, M. Mölle, *Adv. Sci.* **2018**, *5*, 1700038; g) H. Ko, A. Javey, *Acc. Chem. Res.* **2017**, *50*, 691; h) Q. Zhao, Y. H. Liang, L. Ren, Z. L. Yu, Z. H. Zhang, L. Q. Ren, *Nano Energy* **2018**, *51*, 621; i) L. Z. Xu, T. C. Shyu, N. A. Kotov, *ACS Nano* **2017**, *11*, 7587; j) Z. G. Zhao, S. Y. Zhuo, R. C. Fang, L. H. Zhang, X. T. Zhou, Y. C. Xu, J. Q. Zhang, Z. C. Dong, L. Jiang, M. J. Liu, *Adv. Mater.* **2018**, *30*, 1804435; k) G. Stoychev, L. Guiducci, S. Turcaud, J. W. C. Dunlop, L. Ionov, *Adv. Funct. Mater.* **2016**, *26*, 7733; l) L. Ionov, *Mater. Today* **2014**, *17*, 494; m) L. Ionov, *Adv. Funct. Mater.* **2013**, *23*, 4555.

[7] a) Z. J. Wang, C. N. Zhu, W. Hong, Z. L. Wu, Q. Zheng, *Sci. Adv.* **2017**, *3*, e1700348; b) Z. J. Wang, W. Hong, Z. L. Wu, Q. Zheng, *Angew. Chem. Int. Ed.* **2017**, *56*, 15974; *Angew. Chem.* **2017**, *129*, 16190; c) C. M. Gomes, C. Liu, J. A. Paten, S. M. Felton, L. F. Deravi, *Adv. Funct. Mater.* **2019**, *29*, 1805777; d) X. Du, H. Cui, Q. Zhao, J. Wang, H. Chen, Y. Wang, *Research* **2019** https://doi.org/10.1155/2019/6398296; e) T. T. Chen, H. Bakhshi, L. Liu, J. Ji, S. Agarwal, *Adv. Funct. Mater.* **2018**, *28*, 1800514; f) H. Arslan, A. Nojoomi, J. Jeon, K. Yum, *Adv. Sci.* **2019**, *6*, 1800703; g) X. Peng, Y. Li, Q. Zhang, C. Shang, Q.-W. Bai, H. L. Wang, *Adv. Funct. Mater.* **2016**, *26*, 4491; h) Q. Zhao, X. X. Yang, C. X. Ma, D. Chen, H. Bai, T. F. Li, W. Yang, T. Xie, *Mater. Horiz.* **2016**, *3*, 422; i) C. X. Ma, T. F. Li, Q. Zhao, X. X. Yang, J. J. Wu, Y. W. Luo, T. Xie, *Adv. Mater.* **2014**, *26*, 5665.

[8] C. X. Ma, W. Lu, X. X. Yang, J. He, X. X. Le, L. Wang, J. W. Zhang, M. J. Serpe, Y. J. Huang, T. Chen, *Adv. Funct. Mater.* **2018**, *28*, 1704568.

[9] a) C. M. Xie, W. Sun, H. Lu, A. Kretzschmann, J. H. Liu, M. Wagner, H.-J. Butt, X. Deng, S. Wu, *Nat. Commun.* **2018**, *9*, 3842; b) W. Sun, S. Y. Li, B. Haupler, J. Liu, S. B. Jin, W. Steffen, U. S. Schubert, H.-J. Butt, X.-J. Liang, S. Wu, *Adv. Mater.* **2017**, *29*, 1603702; c) M. Martínez-Calvo, O. Kotova, M. E. Möbius, A. P. Bell, T. McCabe, J. J. Boland, T. Gunnlaugsson, *J. Am. Chem. Soc.* **2015**, *137*, 1983; d) Z. Q. Li, G. N. Wang, Y. G. Wang, H. R. Li, *Angew. Chem. Int. Ed.* **2018**, *57*, 2194; *Angew. Chem.* **2018**, *130*, 2216; e) J. Hai, T. R. Li, J. X. Su, W. S. Liu, Y. M. Ju, B. D. Wang, Y. L. Hou, *Angew. Chem. Int. Ed.* **2018**, *57*, 6786; *Angew. Chem.* **2018**, *130*, 6902; f) P. K. Chen, Q. C. Li, S. Grindy, N. Holten-Andersen, *J. Am. Chem. Soc.* **2015**, *137*, 11590; g) G. S. Weng, S. Thanneeru, J. He, *Adv. Mater.* **2018**, *30*, 1706526; h) K. Meng, C. Yao, Q. M. Ma, Z. H. Xue, Y. P. Du, W. G. Liu, D. Y. Yang, *Adv. Sci.* **2019**, *6*, 1802112.

[10] J. S. Renny, L. L. Tomasevich, E. H. Tallmadge, D. B. Collum, *Angew. Chem. Int. Ed.* **2013**, *52*, 11998; *Angew. Chem.* **2013**, *125*, 12218.

[11] a) K. Binnemans, *Chem. Rev.* **2009**, *109*, 4283; b) P. Kumar, S. Soumya, E. Prasad, *ACS Appl. Mater. Interfaces* **2016**, *8*, 8068.

[12] D. Roy, W. L. A. Brooks, B. S. Sumerlin, *Chem. Soc. Rev.* **2013**, *42*, 7214.

[13] D. Stuart-Fox, A. Moussalli, *PLoS Biol.* **2008**, *6*, 22.